Chinese Journal of Chemical Engineering 90 (2026) 203–213

Contents lists available at ScienceDirect

Chinese Journal of Chemical Engineering

journal homepage: www.elsevier.com/locate/CJChE

Full Length Article

Diffusion enhancement for damaged porous media with fractal geometry using a generalized tree-like bifurcation network model

Chijin Zhang [1, 2], Jiawei Teng [2], Chuanming Wang [2, *], Zuwei Liao [1, *], Zaiku Xie [2]

[1] State Key Laboratory of Chemical Engineering and Low-Carbon Technology, College of Chemical and Biological Engineering, Zhejiang University, Hangzhou 310027, China
[2] State Key Laboratory of Green Chemical Engineering and Industrial Catalysis, SINOPEC Shanghai Research Institute of Petrochemical Technology Co., Ltd., Shanghai 201208, China

ARTICLE INFO

Article history:
Received 1 July 2025
Received in revised form
12 September 2025
Accepted 16 September 2025
Available online 28 November 2025

Keywords:
Damaged porous media
Tree-like bifurcation network
Monte Carlo
Diffusion
Fractal geometry

ABSTRACT

The effective diffusion coefficient (EDC) is a fundamental parameter for characterizing gas transport in porous media. Structural damages within the pore network significantly affect the EDC due to the alterations in diffusion pathways. To advance the understanding of these effects, we introduce a novel, physics-based model that explicitly captures the complex morphology of damaged porous structures. Utilizing a generalized tree-like bifurcation network framework combined with Monte Carlo simulations, our approach models gas diffusion according to Fick's law, deriving a comprehensive expression for EDC as a function of critical geometric parameters: porosity, fractal dimension of pore space, surface roughness, connectivity, total branching level, branching angle, and pore damage extent. This methodology eschews empirical assumptions, relying solely on fundamental physical principles, thus ensuring high model fidelity and predictive robustness for complex porous systems. Validation against extensive experimental datasets demonstrates strong agreement, confirming the model's accuracy. Key findings reveal that pore damage shifts the optimal diameter ratio (ODR) from 0.772 into a broader range of 0.788–0.876 under damage scenarios. Moreover, higher branching levels and smaller angles increase the sensitivity of EDC to diameter ratio variations. Tailored pore morphology, particularly in designing different diameter ratios for damaged versus undamaged zones, can significantly enhance gas diffusion efficiency. These results offer a theoretical basis for designing damage-tolerant catalyst porous media during the lifecycle, improving diffusion efficiency by 0.86% to 3.81% compared to traditional designs across three damage models.

1. Introduction

Porous media are solid materials with many interconnected pores, whose size and shape greatly affect properties like permeability, diffusion, and thermal conductivity. Due to their complex and variable structures, such media often exhibit heterogeneity. Early models typically relied on empirical parameters and rarely provided detailed structural information, making the rational design quite challenging. Fractal theory, pioneered by Benoit Mandelbrot [1], provides a powerful framework to describe the inherent complexity and scale-invariance of natural and engineered materials. Unlike Euclidean geometry, which uses integer dimensions for smooth shapes, fractal geometry employs non-integer fractal dimensions to capture irregularity and self-similarity. In gas diffusion, the pore fractal dimension (D_p) quantifies how well the pore space fills the solid materials. A higher D_p indicates a greater abundance of smaller pores contributing significantly to the pore volume and a more complex, tortuous pore network. Based on fractal theory, two primary models are employed to describe porous structures and predict diffusion behavior [2–6]: the capillary bundle model and the tree-like bifurcation network model.

The capillary bundle model represents porous media as a bundle of curved, independent capillary tubes with variable cross-sections that follow a fractal scaling law. Zheng *et al.* [7] derived an analytical expression for the gas diffusion coefficient based on

* Corresponding authors.
E-mail addresses: wangcm.sshy@sinopec.com (C. Wang), liaozw@zju.edu.cn (Z. Liao).

https://doi.org/10.1016/j.cjche.2025.09.033

fractal dimension, porosity, and pore size, confirming its effectiveness for porosities below 0.70. Subsequently, they improved the model's realism and accuracy by discretizing capillary tube sizes using Monte Carlo methods [8]. Yang *et al.* [9] verified the fractal scaling law in shale formation pores through adsorption-desorption experiments and obtained the fractal dimensions from adsorption curves. Their fractal Monte Carlo model showed that, with fixed porosity, increasing the pore fractal dimension reduces apparent and intrinsic permeability but increases the permeability ratio (AGP/IP). Cai *et al.* [10,11] categorized gas flow modes into viscous flow, molecular diffusion and surface diffusion based on the ratio of molecular mean free path to pore size, studying their effects on the apparent permeability of shale gas. Gao *et al.* [12] simulated gas diffusion in fibrous media using converging-diverging capillary bundles, finding that the diffusion coefficient decreases with higher fluctuation amplitude and fluid saturation. Xiao *et al.* [13,14] incorporated surface roughness into the fractal model to better capture heat and mass transfer. Additionally, Li *et al.* [15] combined the capillary bundle model with an evaporation model for describing porous liquid-conducting media, for which the mean relative error was less than 5.98% compared to mercury injection data.

Many studies using the capillary bundle model overlook pore connectivity and branching property, leading to a gap between the model and actual porous media. In contrast, tree-like networks, characterized by branching structure, are common in nature (*e.g.*, plant vascular systems, animal tracheae) and are known for optimal transport efficiency, as shown by Murray [16]. These structures have attracted research across fields such as microchannels [17,18], electronics [19], biology [20,21], and materials science [22]. Research on transport in tree-like networks has evolved: Liu *et al.* [23,24] studied how bifurcation types affect mass and heat transfer, finding that gas diffusion increases with diameter ratio, while thermal conductivity first rises then falls. Besides, larger length ratios reduce both properties. Xiao *et al.* [25,26] examined damage effects in bifurcation networks, analyzing how broken channels and their numbers influence heat and mass transfer. However, these studies focused mainly on single tree-like networks, failing to fully reveal the structure-performance relationship in porous media. Hu *et al.* [27] advanced the work by using a bundle of tortuous fractal tree-like micropore networks to investigate shale permeability and thermal conductivity. Their model, validated against experimental data, highlighted how branching level, angle, length ratio, and diameter ratio affect these properties—particularly emphasizing the significant, positive influence of diameter ratio and the negative impact of length ratio. Other researchers have further refined these models from diverse perspectives. Tang *et al.* [28] constructed a 3D tree-like network inside a sphere to evaluate thermal resistance with various fractal pore structures, providing a foundation for the research on irregular porous media, while Jing *et al.* [29] analyzed how surface charge affects hydraulic resistance in electro-viscous flow within microchannels, showing that solid-liquid interface charge influences the optimal network structure. Liang *et al.* [30] proposed a symmetric polygonal bifurcation network and provided an analytical expression for effective permeability, and Zhang *et al.* [31] investigated heat conduction in dual porous media with asymmetric tree-like bifurcation networks, revealing how porosity and structural parameters affect thermal conductivity.

Although significant advances have been made in tree-like network models, existing approaches exhibit critical limitations that motivate the present study. Most current models assume uniform diameter ratios across all branching levels and fail to consider the need for re-optimization of these ratios when branch channels undergo damage. While Zheng *et al.* [22,32] derived optimal diameter ratios (ODRs) for hierarchical pore structures based on Murray's law, their framework overlooks key microstructural factors such as branching angles, total branching levels, fractal dimensions of the pore space, and the effects of pore damage, due to the simplifying assumption of a constant volumetric flow rate. To overcome these gaps—particularly the lack of damaged structures optimization and the oversimplified treatment of microstructural complexity—this work introduces an innovative model to extend and refine Murray's law. The primary innovation lies in explicitly optimizing diameter ratios separately for undamaged and damaged branches throughout the porous media's lifecycle, thereby enabling more accurate and practical design of tree-like bifurcation networks. Results demonstrate that this strategy significantly enhances mass transfer efficiency in porous media under various damage conditions. The article is structured as follows: Section 2 provides a detailed introduction to the modeling approach; Section 3 validates the model accuracy using literature data; Section 4 discusses the effects of different structural parameters on diffusion, and Section 5 presents the conclusions.

2. Methodologies

2.1. Tree-like bifurcation network

Fig. 1 depicts the tree-like bifurcation network model used to represent the pore structure of a porous medium. Within this model, k denotes the branching level index. At $k = 0$, this corresponds to the parent tubes, and $k > 0$ indicates the sub-tubes. Key geometric parameters are defined as follows: θ is the branching angle, uniform across all bifurcation points; d_k and l_k represent the diameter and length of the tubes at level k, respectively. And L_0 signifies the effective diffusion length within the porous medium. The model incorporates the following structural assumptions: First, at each successive level $(k+1)$, the number of branches doubles relative to the preceding level (k), establishing a constant branching number $n = 2$. Second, to ensure physical realism and avoid overlap between adjacent sub-tubes, both the total volume occupied by the network and the branching angle θ are constrained to finite values. Finally, the size distribution of the parent tubes $(k = 0)$ follows fractal scaling. The cumulative number N of parent tubes with diameter greater than or equal to d_0 is governed by Eq. (1). Given the minimum $(d_{0,\min})$ and maximum $(d_{0,\max})$ diameters of parent tubes, the total number of distinct tree-like networks N_T within the representative volume is given by: $(d_{0,\max}/d_{0,\min})^{D_p}$, where D_p is the pore fractal dimension. Consequently, the probability density function for parent tubes diameters within the range d_0 to $d_0 + \Delta d_0$ is described by Eq. (2).

$$N(d_0) = \left(d_{0,\max}/d_0\right)^{D_p} \tag{1}$$

$$-\Delta N(d_0) \Big/ N_T = D_p d_{0,\min}^{D_p} d_0^{-D_p-1} \Delta d_0 = f(d_0)\Delta d_0 \tag{2}$$

Building upon the fractal scaling defined by Eq. (2), the diameter ratio of the parent tubes ($d_{0,\min}$/ $d_{0,\max}$) is constrained to be less than 0.01. This condition ensures the statistical validity of the fractal size distribution. Consequently, the cumulative probability distribution function (CDF) for the parent tube diameter is derived as Eq. (4).

$$\int_{d_{0,\min}}^{d_{0,\max}} f(d_0)\Delta d_0 = 1 - \left(\frac{d_{0,\min}}{d_{0,\max}}\right)^{D_p} \equiv 1 \Longrightarrow d_{0,\min} \Big/ d_{0,\max} \le 0.01 \tag{3}$$

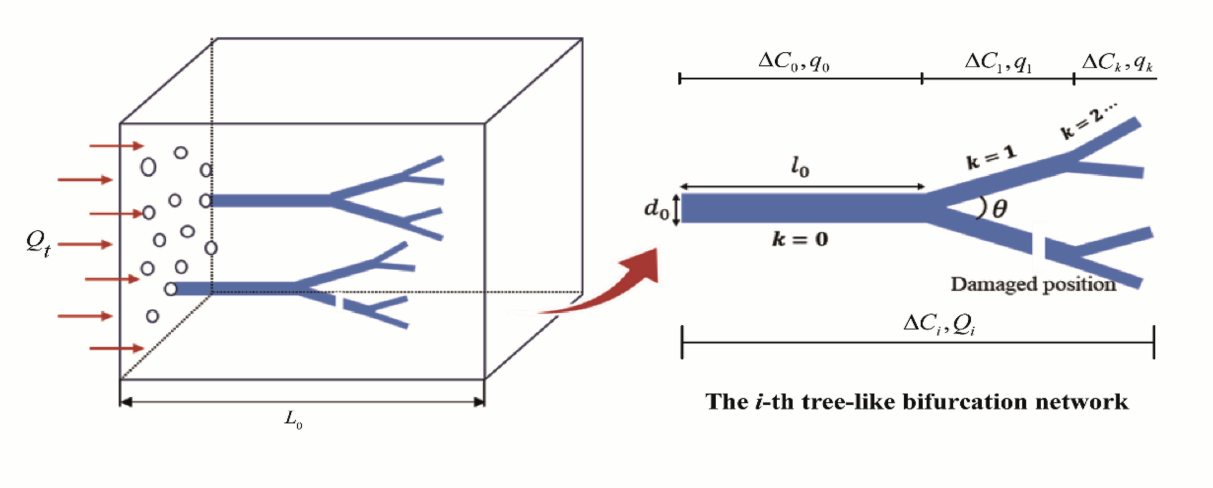

Fig. 1. Diagram of tree-like bifurcation network structure.

$$R(d_0) = \int_{d_{0,\min}}^{d_0} f(d_0)\Delta d_0 = 1 - (d_{0,\min}/d_0)^{D_p} \in (0,1) \tag{4}$$

To represent the pore structure of realistic porous media, we generate ensembles of tree-like bifurcation networks with Monte Carlo method, which ensures the discreteness of the tube diameter and is often used in reported fractal models [8,9,13,14]. The implementation proceeds as follows:

(1) **Parent-tube diameter assignment:** For the i-th tree-like bifurcation network, generate a uniformly distributed random number $R_i \in (0,1)$. The corresponding parent-tube diameter is calculated *via* Eq. (5), which comes from Eqs. (3) and (4):

$$d_{0,i} = d_{0,\min} \Big/ (1 - R_i)^{1/D_p} \tag{5}$$

(2) **Sub-tubes network construction:** For a given network, the length and diameter of sub-tubes ($k > 0$) derive from parent tube *via* level-dependent ratios: $\alpha(k) = l_{k+1}/l_k$ and $\beta(k) = d_{k+1}/d_k$, in which l_0 is set by the user-input. The total horizontal length and vertical height of the network are given by Eq. (6a) and (6b), and m is the total branching levels.

$$L_0 = l_0 + \sum_{k=1}^{m} l_k \cdot \cos\theta \tag{6a}$$

$$H_0 = d_0 + \sum_{k=1}^{m} 2l_k \cdot \sin\theta \tag{6b}$$

(3) **Pore volume calculation:** Total pore volume (V) of the porous medium, represented by N_T tree-like networks, is equal to the sum of the sub-volume (V_i) of each tree-like network (Eq. (7)). Damage within each network is characterized by two parameters: the branching level k_d, where damage occurs, and the number of damaged branches N_d at this level, with $0 \le N_d \le n^{k_d}$. When k is less than k_d, the tree-like network branches are not damaged, and the pore volume is $\sum_{k=0}^{k_d-1} \pi d_k^2 l_k n^k/4$; When k is greater than k_d, the corresponding pore volume is $\sum_{k=k_d}^{m} \pi d_k^2 l_k \left(n^k - N_d n^{k-k_d}\right)/4$ by removing the damaged branches. Therefore, the sub-volume of each tree-like network associated with damaged channels is determined by Eq. (8). Here, $N_d = 0$ indicates an undamaged porous structure, whereas $N_d = n^{k_d}$ signifies complete blockage of the pores at the affected level, completely preventing gas flow through the medium.

$$V = \sum_{i=1}^{N_T} V_i \tag{7}$$

$$V_i = \sum_{k=0}^{k_d-1} \pi d_k^2 l_k n^k \Big/ 4 + \sum_{k=k_d}^{m} \pi d_k^2 l_k \left(n^k - N_d n^{k-k_d}\right) \Big/ 4 \tag{8}$$

(4) **Diffusion cross-sectional area calculation:** The effective cross-sectional area A_t for diffusion is calculated using the total pore volume V, volume-porosity ϕ_v, and the effective diffusion length L_0, Noting that the effective diffusion length of the porous medium is the maximum value of the total horizontal length among all tree-like bifurcation networks.

$$A_t = V / (\phi_v L_0) \tag{9}$$

2.2. Formula of effective diffusion coefficient

Gas diffusion in porous media varies primarily with pore size and includes molecular diffusion, Knudsen diffusion, and surface diffusion. The pore sizes considered in this paper are large enough and the diffusion behavior occurs under room temperature, therefore the phenomenon of gas adsorption is not significant and the influence of surface diffusion is neglected. The dominant type of diffusion is determined by the Knudsen number (Kn), defined as the ratio of the molecular mean free path (λ) to the pore diameter (d_k).

$$Kn = \lambda/d_k \tag{10}$$

Where the mean free path is given by $\lambda = k_B T/\left(\sqrt{2}\,\pi P \sigma^2\right)$. k_B is the Boltzmann constant ($k_B = 1.3806 \times 10^{-23}$ J·K^{-1}), T is temperature, K, P is pressure, Pa, σ is the gas molecule diameter, m.

When the Knudsen number $Kn > 10$, Knudsen diffusion predominantly governs the mass transfer process, and the diffusion coefficient for a k-th cylindrical tube (D_k) is calculated using Eq. (11a) [33]. Conversely, for $Kn < 0.1$, molecular diffusion becomes

the dominant mechanism, with the corresponding diffusion coefficient determined by Eq. (11b) [34]. In the intermediate regime where $0.1 \le Kn \le 10$, both Knudsen and molecular diffusion mechanisms influence the mass transfer process simultaneously. In this case, the effective diffusion coefficient is computed using Eq. (11c) [35]. Notably, as the pore diameter d_k increases or decreases, Eq. (11c) can be transformed into either Eq. (11b) or (11a).

$$D_k = \begin{cases} \dfrac{2\sqrt{2}d_k k_B^{0.5} T^{0.5}}{3\pi^{0.5} M^{0.5}}, Kn > 10 & (11a) \\ \dfrac{2k_B^{1.5} T^{1.5}}{3\pi^{1.5}\sigma^2 P M^{0.5}}, Kn < 0.1 & (11b) \\ \dfrac{2k_B^{1.5} T^{1.5}}{3\pi^{1.5}\sigma^2 P M^{0.5}} \left[1 - \exp\left(-\dfrac{d_k}{\lambda}\right)\right], 0.1 \le Kn \le 10 & (11c) \end{cases}$$

Where M stands for the gas molecular mass, kg.

Assume that Q_i is the total flow through the i-th tree-like bifurcated network, then the volumetric flow q_k through a branch at level k is obtained by the ratio of Q_i to the number of branches. When the branch is intact, $q_k = Q_i/n^k, k < k_d$; conversely, if the branch is damaged, $q_k = Q_i/\left(n^k - N_d n^{k-k_d}\right), k \ge k_d$. Besides, q_k can also be calculated based on Fick's diffusion law, as shown in Eq. (12). Therefore, concentration difference ΔC_k is obtained by Eq. (13), accounting for whether there are damaged pores or not.

$$q_k = \frac{\pi d_k^2 D_k}{4} \frac{\Delta C_k}{l_k} \tag{12}$$

$$\Delta C_k = \begin{cases} \dfrac{4Q_i l_k}{\pi d_k^2 D_k} \cdot \dfrac{1}{n^k}, k < k_d \\ \dfrac{4Q_i l_k}{\pi d_k^2 D_k} \cdot \dfrac{1}{\left(n^k - N_d n^{k-k_d}\right)}, k \ge k_d \end{cases} \tag{13}$$

The total concentration drops ΔC_i across the entire network i (from inlet at $k = 0$ to outlets at $k = m$) is the sum of the concentration differences along single tube (Eq. (14)). Combining Eqs. (12)–(14) yields the relationship between the total flow rate Q_i entering i-th network and its concentration drop ΔC_i (Eq. (15)). Since all tree-like networks within the representative volume experience the same overall concentration difference between their inlets and outlets ($\Delta C_1 = \Delta C_2 = \cdots = \Delta C_{N_T} = \Delta C$), the total gas flow rate through the porous medium is $Q_t = \sum_{i=1}^{N_T} Q_i$. Applying Fick's diffusion law macroscopically to the entire porous medium (using effective properties A_t, L_0 and ΔC) provides the expression for the EDC (Eq. (16)).

$$\Delta C_i = \sum_{k=0}^{m} \Delta C_k = \sum_{k=0}^{k_d-1} \frac{4Q_i l_k}{n^k \pi d_k^2 D_k} + \sum_{k=k_d}^{m} \frac{4Q_i l_k}{\pi d_k^2 D_k} \cdot \frac{1}{\left(n^k - N_d n^{k-k_d}\right)} \tag{14}$$

$$Q_i = \Delta C_i \Bigg/ \left[\sum_{k=0}^{k_d-1} \frac{4l_k}{n^k \pi d_k^2 D_k} + \sum_{k=k_d}^{m} \frac{4l_k}{\pi d_k^2 D_k} \cdot \frac{1}{\left(n^k - N_d n^{k-k_d}\right)} \right] \tag{15}$$

$$D_e = \frac{Q_t L_0}{A_t \Delta C} = \frac{L_0}{A_t} \sum_{i=1}^{N_T} \frac{1}{\sum_{k=0}^{k_d-1} \frac{4l_k}{n^k \pi d_k^2 D_k} + \sum_{k=k_d}^{m} \frac{4l_k}{\pi d_k^2 D_k} \cdot \frac{1}{\left(n^k - N_d n^{k-k_d}\right)}} \tag{16}$$

The core diffusion model described above, based on idealized tree-like networks, neglects three key microstructural features influencing gas diffusion: pore roughness, tortuosity and interconnectivity between parent tubes. We incorporate these effects based on established physical principles. Following Yang *et al.* [36], the relative roughness ε_k of a capillary is defined using a fractal roughness element model as the ratio of the average roughness height to the nominal diameter: $\varepsilon_k = \overline{h}/d_k$. The effective diameter accounting for roughness is given by $d_k^{\text{eff}} = d_k(1 - \varepsilon_k)$. Adopting the fractal-based expression from Yu *et al.* [37], tortuosity for a curved tube is a function of the tortuosity fractal dimension D_t, the pore diameter, and the straight-section length, the expression is shown as $\tau_k = d_k^{1-D_t} l_k^{D_t-1}$. Furthermore, connectivity between parent tubes is modeled probabilistically, assuming a normal distribution described by the probability density function in Eq. (17), where c stands for the connectivity, δ_c is the standard deviation, and μ_c is the average value of connectivity. These microstructural factors modify the local diffusion coefficient within a channel. Their combined influence is incorporated *via* the relationship defined as $D_k^{\text{eff}} = D_k c/\tau_k^2$ with $c = 1$ for $k > 0$.

$$f(c) = \frac{1}{\sqrt{2\pi}\delta_c} \exp\left[-\frac{(c - \mu_c)^2}{2\delta_c^2} \right] \tag{17}$$

3. Model Validation

To validate the diffusion model for a single tree-like bifurcation network ($N_T = 1$), we simulated the effective diffusion coefficient (EDC) of oxygen molecules at 293 K and 0.1 MPa, investigating its dependence on network structural evolution. Simulation results were benchmarked against literature data [25], as shown in Fig. 2. The primary model parameters are $d_0 = 1$ μm, $l_0 = 10$ μm for parent tube, branching angle and branching number are 45° and 2, damaged branching level k_d is 2. Dimensionless EDC ($D_e^+ = D_e/D_0$) is plotted against key structural parameters, where $D_0 = 1.8 \times 10^{-5}$ $m^2 \cdot s^{-1}$. According to Fig.2(a), D_e^+ exhibits a monotonic increase with increasing D_d. Notably, the rate of increase is highest at lower D_d values and diminishes as D_d increases. The fractal dimension D_d governs the scaling relationship $n = \beta^{-D_d}$. In contrast, increasing D_l or m causes D_e^+ to decrease sharply initially, followed by gradual stabilization at larger values. The scaling $n = \alpha^{-D_l}$ defines the length fractal dimension D_l. The results shows that proposed model effectively captures the EDC under damaged conditions ($N_d = 0, 2, 3$), showing good agreement with the reference data (scatter points) across all parameter variations.

To represent realistic porous media, we employ an ensemble of $N_T \gg 1$ tree-like bifurcation networks. We simulated hydrogen diffusion (293 K, 0.1 MPa) across varying porosities and assessed model convergence and predictive capability against experimental data [38]. Simulation conditions mirrored the experiment: zero total branching level ($m = 0$), reducing the pore structure to parallel capillaries with diameters ranging from 90 nm to 90 μm. Fractal dimensions were calculated using established correlations (Eqs. (18) [39] and (19) [40]). Fig. 3(a) shows the dependence of the predicted EDC on N_T. At low N_T values, predicted EDC exhibits significant statistical fluctuations. The fluctuation amplitude increases with higher porosity, reflecting greater structural variability inadequately sampled by small ensembles. As N_T increases, the predictions gradually stabilize, reaching a steady state when N_T exceeds 1.0×10^6. Recognizing the critical role of connectivity between parent tubes, we simulated EDC for connectivity parameters $c = 1$ and $c = 2$ across the porosity range. According to Fig. 3(b), the computational results encompass experimental

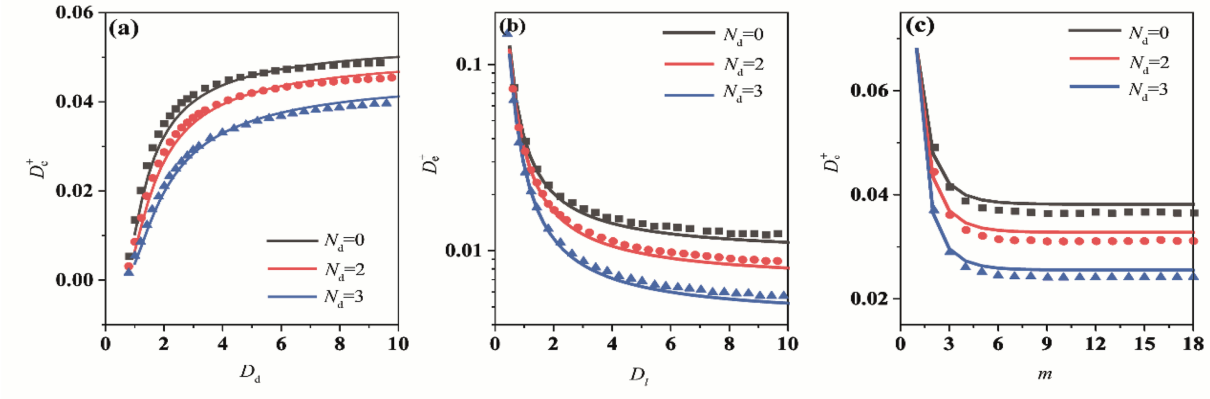

Fig. 2. Evolution of dimensionless EDC with network structure (a) D_d; (b) D_l; (c) total branching level ($d_0 = 1\ \mu m, l_0 = 10\ \mu m, \theta = 45°, n = 2, k_d = 2$).

data from various porous materials with connectivity ranging from 1 to 2, further validating the effectiveness of the proposed model.

$$D_p = d_e - \frac{\ln(\phi_v)}{\ln\left(\frac{d_{0,min}}{d_{0,max}}\right)} \tag{18}$$

$$D_t = 1 + \frac{\ln(\overline{\tau})}{\ln\left(\frac{l_0}{\overline{d_0}}\right)} \tag{19}$$

Where d_e is a geometric dimension constant ($d_e = 3$ in this work), ϕ_v is volume porosity in three-dimensional space, $\overline{\tau}$ is average tortuosity with $\overline{\tau} = 1 + 0.63\ln(1/\phi_v)$ [41], $\overline{d_0}$ is average diameter of parent tube with $\overline{d_0} = D_p d_{0,min}/(D_p - 1)$ [42].

4. Results and Discussion

Leveraging our novel mathematical model, we methodically investigate how pore architecture governs the EDC in damaged tree-like bifurcation networks. Primary factors include pore fractal dimension, total branching levels, and branching angles. Crucially, we establish a rigorous optimization framework for the diameter ratio (β) under damaged conditions to maximize mass transfer efficiency. Our simulations reveal that conventional Murray's law ($ODR^{Murray} = 0.758$) requires significant modification when damage occurs. All simulations adopt baseline parameters from Table 1 unless otherwise specified. The convergence-validated model provides actionable guidelines for fabricating damage-tolerant porous materials in catalytic substrates and energy storage systems.

Table 1
Model parameters and default values.

Items	Default value	Items	Default value
T	293 K	n	2.0
P	101325 Pa	$d_{0,max}$	90 μm
σ	2.74×10^{-10} m	$d_{0,min}$	90 nm
M	3.2226×10^{-27} kg	l_0	400 μm
α	0.6	N_T	2×10^6
β	0.6	ϕ_v	0.5
θ	30°	ε_k	0.05
m	3	(μ_c, δ_c)	(1.2, 0.1)

4.1. Undamaged network design

Building upon Zhou *et al.*'s [32] application of Murray's law to porous structures, our analysis confirms that cylindrical tree-like bifurcation networks governed by Knudsen diffusion obey the diameter proportionality $\sum r_0^{2.5} = \sum r_1^{2.5} = \sum r_2^{2.5}$ across branching levels. When the branching number of the network is equal to 2.0, the optimal diameter ratio (ODR) calculated from Murray's law for an undamaged network is approximately 0.758. Using the parameters in Table 1, we simulated hydrogen diffusion across

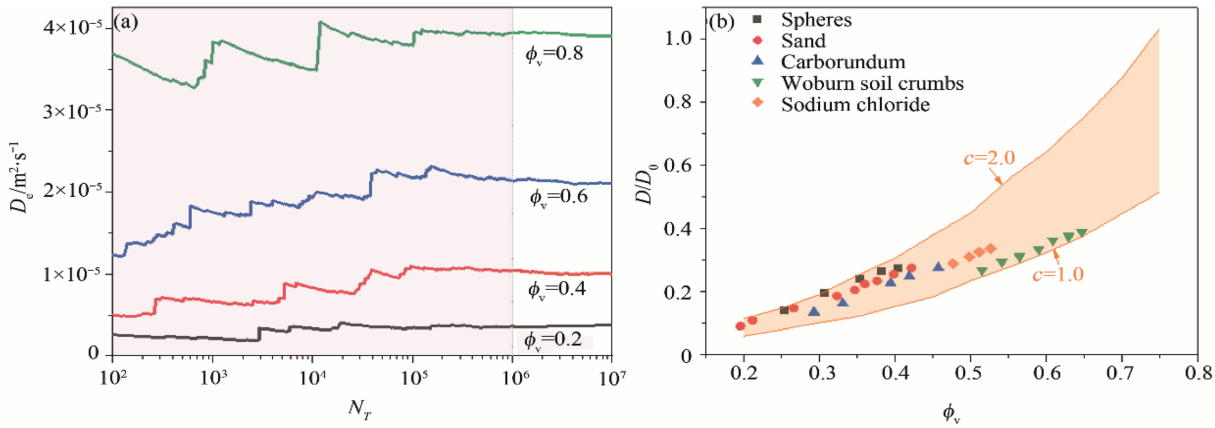

Fig. 3. Model testing for (a) convergence; (b) effectiveness ($D_0 = 6.51 \times 10^{-5}\ m^2 \cdot s^{-1}, d_{0,min} = 90\ nm, d_{0,max} = 90\ \mu m, m = 0$).

varying porosities and diameter ratios (Fig. 4(a)). When $\beta < 0.4$, third-level branches reach critical diameters of 5.0 nm, inducing Knudsen-dominated diffusion where effective diffusion coefficients (EDCs) converge below 2.5×10^{-6} $m^2 \cdot s^{-1}$ regardless of porosity. As the diameter ratio increases beyond this threshold, the EDC initially rises, reaches a peak at approximately 0.772, consistent with the ODR predicted by Murray's law, and then declines. Statistical sampling of 4000 Knudsen numbers (Kn) from two million tree-like networks (Fig. 4(b)) reveals that the diffusion type is mainly Knudsen diffusion and molecular diffusion ($0.1 < Kn < 10$) in sub-tubes and parent tubes. This bimodal diffusion regime explains the slight deviation between our simulated ODR and literature values, as Murray's law assumes a single diffusion type.

4.2. Pore fractal dimension

The fractal dimension of the pore structure, D_p, governs the pore diameter distribution *via* Eq. (1), directly influencing the effective diffusion coefficient of gases. Fig. 5(a) presents simulation results conducted with a constant tortuosity fractal dimension, $D_t = 1.1$, which affects the diffusion path length. Under the same D_p, larger tube diameters correspond to a smaller fraction of such pores, whereas increasing D_p promotes a higher prevalence of small-diameter parent tubes. These microstructural changes increase the overall diffusion resistance, leading to a systematic decrease in the EDC across all diameter ratios, as shown in Fig. 5(b). Analyzing the evolution of the EDC with D_p at four different diameter ratios reveals that the maximum EDC consistently occurs at a diameter ratio $\beta = 0.75$, regardless of D_p variation, and the minimum EDC occurs at a diameter ratio of 0.85, which deviates most from 0.75. Combining this with our research content in Section 4.1, it can be inferred that the optimal diameter ratio (ODR) for maximizing gas diffusion efficiency remains largely independent of the pore fractal dimension.

4.3. Total branching level and angle

In porous media, both the total branching level and the branching angle of a tree-like network affect the diffusion rate of gas molecules, thereby altering the ODR. Fig. 6(a) illustrates a heatmap of the EDC under different branching levels and diameter ratios. When the total branching level of the tree-like network is low ($m < 4$), the diameter ratio has less impact on the EDC, resulting in a wider range that allows gas to diffuse rapidly within the porous medium. As the total branching level increases, the size of the terminal branches at lower diameter ratios reaches a critical value that restricts diffusion, leading to a higher diffusion resistance throughout the network, and a narrowing of the ODR range. Fig. 6(b) shows the combined effects of branching angle and diameter ratio on the EDC. It can be observed that when the diameter ratio is below 0.4, the influence of the branching angle on the EDC is negligible, with the EDC of gas under any branching angle remaining below 1.0×10^{-6} $m^2 \cdot s^{-1}$. As the diameter ratio increases, lower branching angles become more favorable for the diffusion of gas molecules. With a gradual increase in branching angle, the diffusion path in the vertical direction expands, resulting in increased resistance to horizontal diffusion of the gas, which leads to a gradual decrease in its EDC within the porous medium.

4.4. Damaged network design

To evaluate Murray's law applicability in damaged systems, we systematically analyzed diameter power sums ($\sum d_k^{2.5}$) across branching levels under varying diameter ratios (β), with the outcomes illustrated in Fig. 7. In intact networks (Fig. 7(a)), curves intersect at $\beta = 0.772$, satisfying Murray's optimization criterion. When $\beta < 0.772$, proximal branches (lower k) exhibit greater $\sum d_k^{2.5}$ than distal branches (higher k), making terminal branch diameters the dominant flow constraint. When $\beta > 0.772$, reduced $\sum d_k^{2.5}$ in proximal branches shifts flow limitation to parent tube dimensions. This shows that the physical meaning of the optimal diameter ratio is to make the pores at different levels have the same or similar gas flow capacity. However, when localized damage occurs at level $k_d = 3$, the tube size of which is the smallest in the entire network, a loss of diffusion pathways eliminates curve intersection (Fig. 7(b)), demonstrating the inapplicability of Murray's law to compromised porous media.

For damaged tree-like bifurcation networks, we propose two optimization approaches by considering whether the diameter ratio is variable or not.

(1) **Uniform diameter ratio optimization:** maintaining the same β across levels, increasing damaged branches N_d preserves unimodal EDC distribution (Fig. 8(a)). In this section, the damaged branch level k_d is 3, and the number of damaged branches N_d of 2, 4, and 6 corresponds to damage ratios of 25%, 50% and 75% for porous media. Simulation results reveal that ODR increases from 0.788 to 0.876 with rising N_d, and the maximum EDCs exceed Murray's law predictions by 12% to 18% (as shown in Table 2).

(2) **Tiered differential optimization:** Allowing distinct β values for damaged ($k = 3$) and intact ($k < 3$) levels (Fig. 8(b)–(d)) induces systematic migration of the EDC maximum. As N_d increases, the region of maximum EDC shifts upward and exhibits contraction. This phenomenon reveals a core compensation mechanism: enlarging pores adjacent to damaged channels counterbalances localized flow

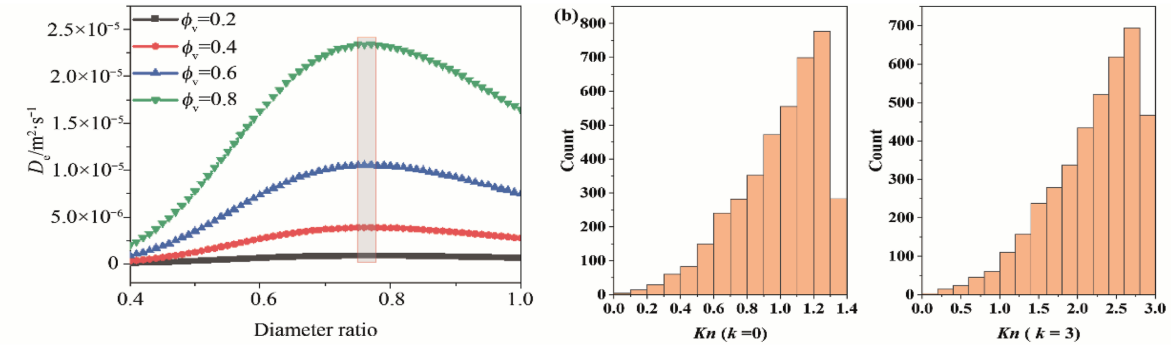

Fig. 4. Simulation results (a) Effect of diameter ratio; (b) Knudsen number with $\phi_v = 0.6, \beta = 0.772$.

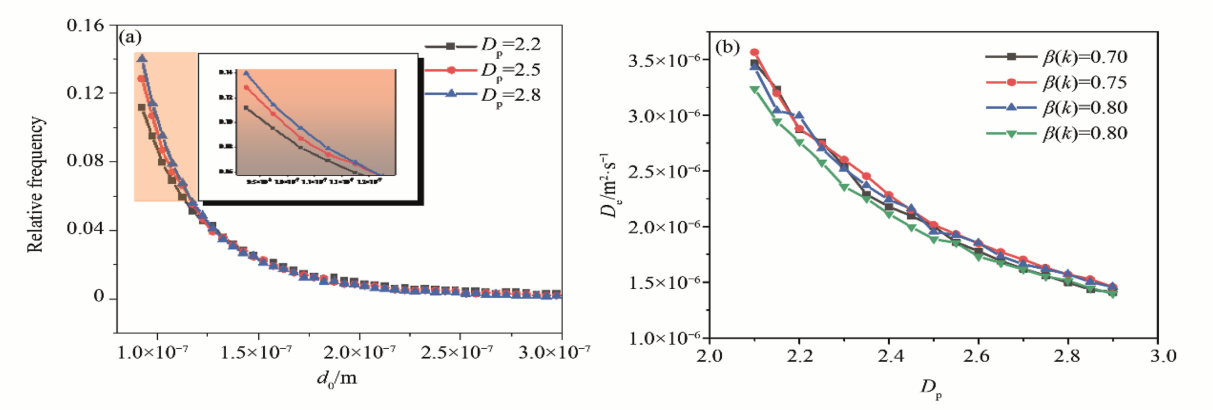

Fig. 5. (a) Parent tube diameter distribution and (b) Effective diffusion coefficient under different pore fractal dimensions with $D_t = 1.1$.

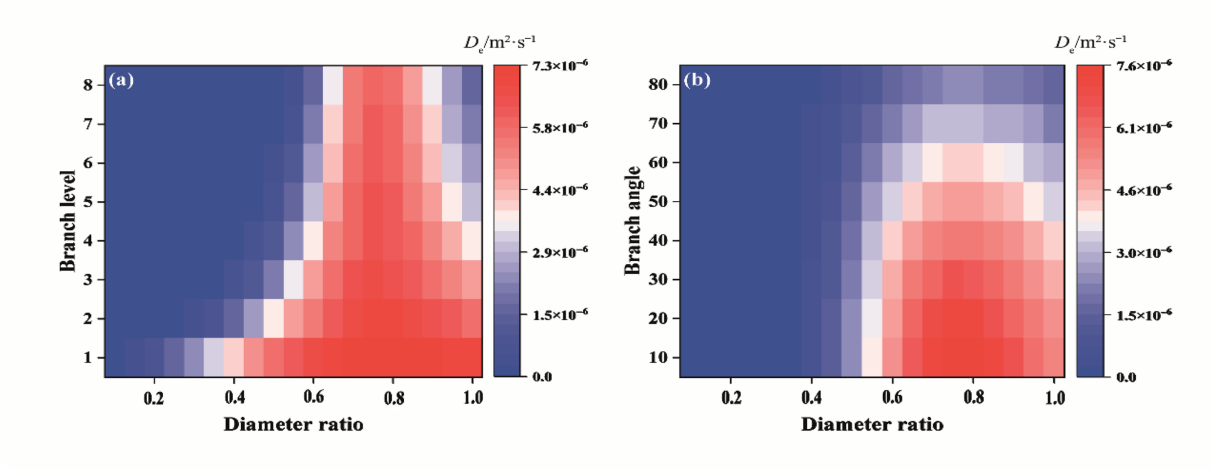

Fig. 6. Heatmap of effective diffusion coefficient with (a) total branching level; (b) branching angle ($d_{0,min} = 90$ nm, $d_{0,max} = 90$ μm, $l_0 = 400$ μm).

resistance surges. This tiered optimization strategy establishes a new paradigm for damage-tolerant porous material design. As detailed in Table 2, when N_d increases to 2, 4, and 6, the ODR for damaged branches increases from 0.768 to 1.0, and the corresponding EDCs significantly exceed the maximum value under uniform diameter ratio conditions. Notably, the EDCs obtained using these methods are higher than those from designs following Murray's law.

Considering the same damage scenario (50% damage at the end level, $k_d = 3$, $N_d = 4$), the effects of porosity, relative roughness,

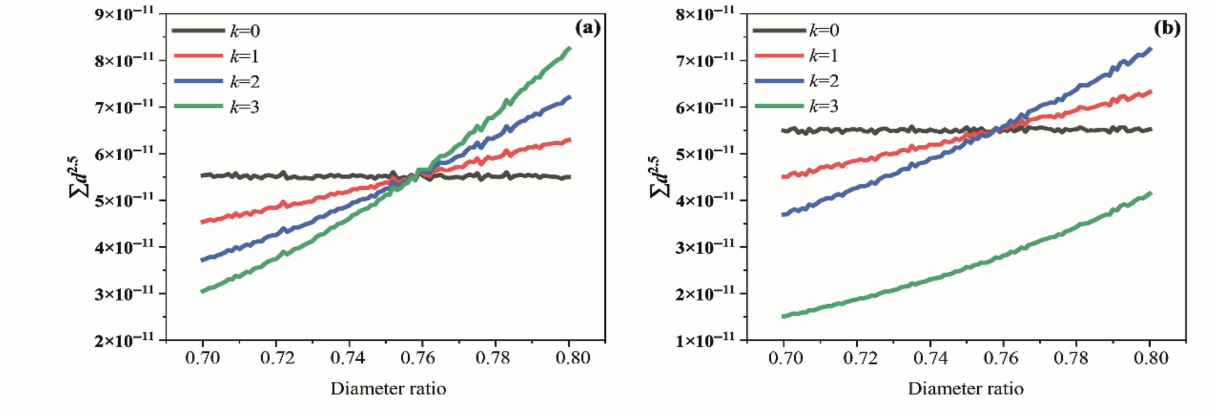

Fig. 7. The sum of branch diameter powers at different diameter ratios in (a) non-damaged tree-like network; (b) damaged tree-like network with $k_d = 3$, $N_d = 4$.

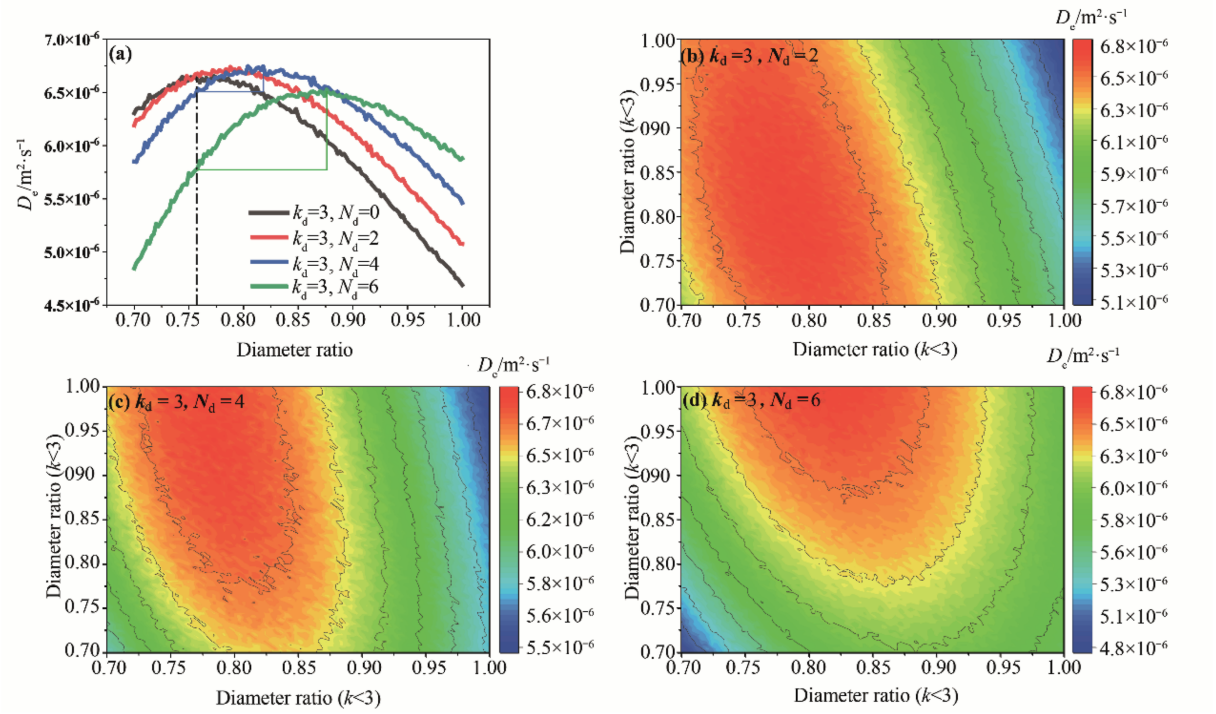

Fig. 8. Effective diffusion coefficient optimization in damaged tree-like network with (a) uniform diameter ratio; (b)–(d) tiered differential diameter ratio.

Table 2
Design results of ODR for damaged tree-like networks.

Cases	Murray law	Uniform diameter ratio		Tiered differential diameter ratio		
	EDC/m^2·s^{-1}	ODR	EDC/m^2·s^{-1}	ODR (k < 3)	ODR (k = 3)	EDC/m^2·s^{-1}
k_d = 3, N_d = 0	6.619 × 10^{-6}	0.772	6.658 × 10^{-6}	–		
k_d = 3, N_d = 2	6.665 × 10^{-6}	0.788	6.741 × 10^{-6}	0.80	0.768	6.751 × 10^{-6}
k_d = 3, N_d = 4	6.587 × 10^{-6}	0.814	6.748 × 10^{-6}	0.776	0.932	6.839 × 10^{-6}
k_d = 3, N_d = 6	5.923 × 10^{-6}	0.876	6.527 × 10^{-6}	0.788	1.0	6.788 × 10^{-6}

and connectivity on the D_e^{opt} and ODR determined by uniform diameter ratio optimization are investigated. Fig. 9(a)–(c) reveal monotonic dependencies of the optimum effective diffusion coefficient (D_e^{opt}) on three structural parameters, which increases linearly with pore connectivity and decays gradually with relative roughness. As for porosity, D_e^{opt} show a gradual initial rise followed by accelerated growth above ϕ_v = 0.50. Crucially, statistics of the optimal diameter ratio under diverse configurations, the diameter ratios maximizing EDC converge narrowly to 0.81–0.82 (Fig. 9(d)), which is similar to the values in Table 2 (equal to 0.814). This phenomenon suggests that pore damage is the primary factor influencing the optimal diameter ratio.

4.5. Catalyst structure design during lifecycle

In gas-solid phase reactions, catalyst deactivation often occurs due to coke deposition, which damages pore structures and reduces mass transport efficiency. A critical limitation in conventional industrial catalyst design is the neglect of progressive pore blockage, resulting in local optimal structural configurations over the catalyst's lifecycle. To address this, we introduce a time-dependent damage probability function, $\Psi(t)$, quantifying the likelihood of pore damage within a porous medium comprising N_t tree-like networks. By simulating the diffusion of gas in porous media with different degrees of damage under different structural parameters, the cumulative diffusion flux per unit area (Q) is calculated to screen out the optimal structure, which is defined as the time integral of the effective diffusion coefficient ($Q = \int D_e dt$). Using the model parameters specified in Table 1 (with k_d = 3, N_d = 6), we examine three distinct $\Psi(t)$ trends (Fig. 10(a)). Here, $\Psi(t) = 0$ represents an undamaged pore structure, while $\Psi(t) = 1$ corresponds to 75% pore blockage. Fig. 10(b) illustrates the evolution of D_e over 100 days for a catalyst designed with the conventional "optimal diameter ratio" (ODR = 0.772), which disregards pore blockage. For a nonlinear increasing $\Psi(t)$ with a slower growth rate in the initial stage (Nonlinear 1), D_e remains at a high level, yielding the highest Q (55.37 m^2) over 100 days. Conversely, when $\Psi(t)$ exhibits rapid initial growth followed by slower progression (Nonlinear 2), D_e declines rapidly in the early stage, resulting in the lowest Q (53.43 m^2). To identify the true lifecycle-optimal pore geometry, we systematically evaluate diameter ratios and their associated Q values (Fig. 10(c)). The analysis demonstrates that tailored diameter ratios can compensate for damage trends, achieving comparable diffusion performance across all three $\Psi(t)$ scenarios. In this study, the optimized diameter ratios are 0.820 (Linear), 0.795 (Nonlinear 1), and 0.835 (Nonlinear 2), with corresponding Q improvements of 1.98%,

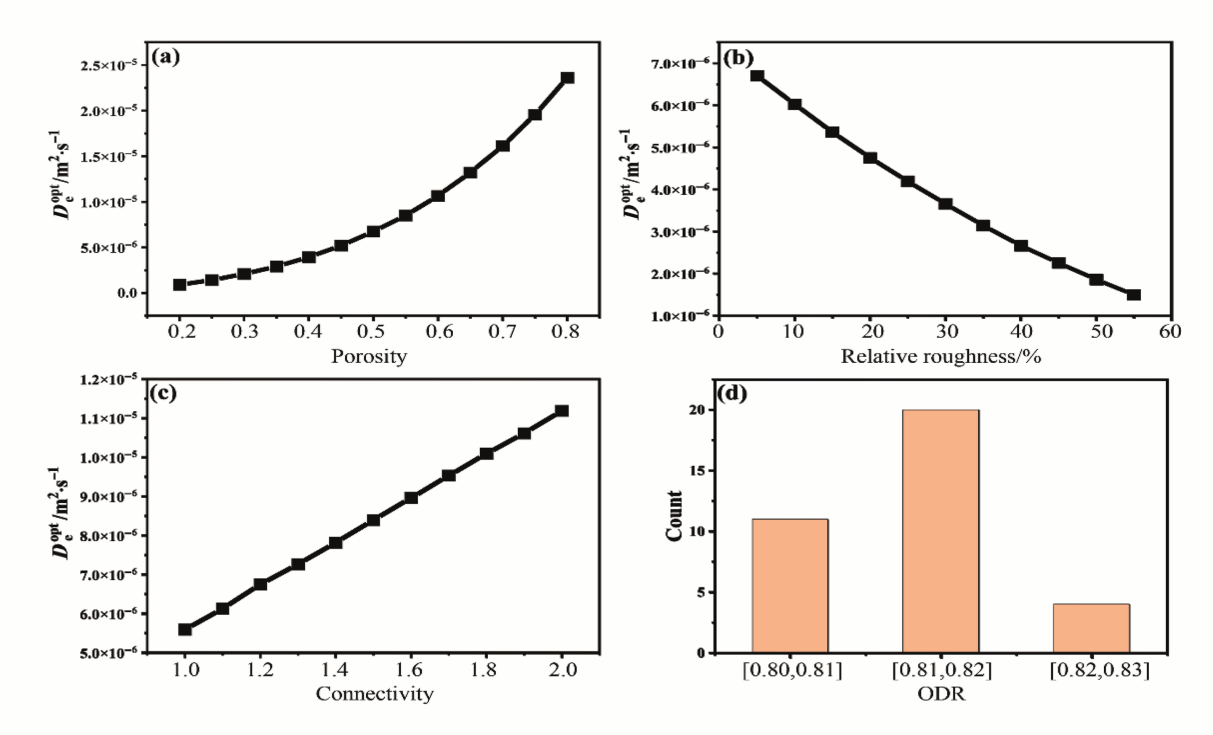

Fig. 9. Optimal effective diffusion coefficient under different structural parameters (a) porosity; (b) relative roughness; (c) connectivity and (d) statistically optimal diameter ratio.

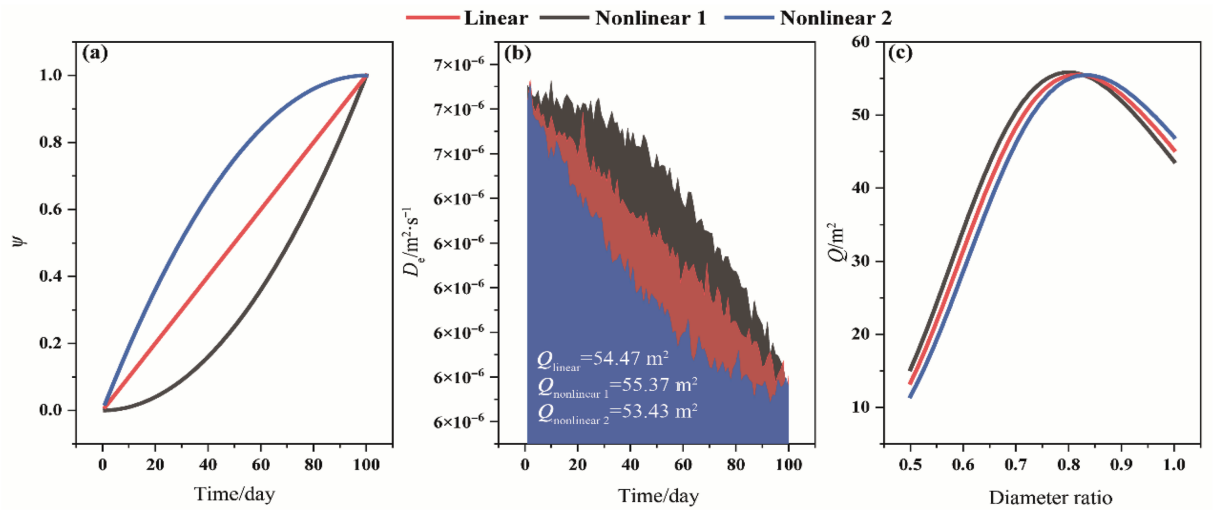

Fig. 10. Catalyst structure design during lifecycle (a) damage probability curves (b) EDC with time (c) cumulative diffusion flux per unit area *vs.* diameter ratio.

0.86%, and 3.81% compared with the traditional design (ODR = 0.772), respectively. This approach enables robust catalyst design by explicitly incorporating time-dependent structural damage, ensuring sustained high diffusion efficiency throughout operational lifespans.

5. Conclusions

This study employs a tree-like bifurcation network to effectively characterize the irregularity, self-similarity, and space-filling properties to porous media. By integrating this network model with a Fick's diffusion law, we develop a comprehensive framework for predicting effective diffusion coefficients based entirely on physical parameters. Under identical conditions, the predictions generated by our model show good agreement with existing reference data from the literature. Systematic comparisons of structural parameters, including pore fractal dimension, total branching levels, diameter ratio, and bifurcation angles, lead to the following key conclusions:

(1) In the proposed model framework, the diameter of the parent-tube is determined by the Monte Carlo method. When there is no damage in tree-like networks, the ODR making a maximum EDC is 0.772, which deviates slightly

from the value of 0.758 obtained by Murray's law. The reason is that the diffusion types in part branches include both Knudsen diffusion and molecular diffusion, while Murray's law only considers a single category of diffusion. In addition, a comparison of EDC under different pore fractal dimensions revealed that, although it affects the distribution of pore size, it hardly changes the ODR.

(2) The total branching level and branch angle have a significant impact on EDC. When the total branching level is less than 4.0, the range of diameter ratios corresponding to high EDCs is broader. Increasing the total branching level causes the overall diffusion resistance of the network to rise, thereby narrowing the range. When the diameter ratio is less than 0.4, the influence of branch angles on EDC can be neglected. As the diameter ratio increases, smaller branch angles result in higher EDCs.

(3) When a tree-like network sustains damage, the predictive accuracy of Murray's law for the ODR diminishes. To address this, two optimization strategies were employed, considering whether the diameter ratios of individual branches are uniform or not. In the case of uniform diameter ratios, the EDC exhibits a unimodal distribution with respect to the diameter ratio. The ODR corresponding to the maximum EDC increases from 0.788 to 0.876 as the extent of damage escalates from 25% to 75%. This observation suggests a core compensation mechanism: enhancing the pore size near damaged branches can counterbalance the increased local mass transfer resistance. Conversely, a tiered differential optimization method is applied when considering distinct diameter ratios for intact and damaged branches. The results demonstrate that the EDC achieved through this approach markedly surpasses the values obtained under uniform diameter ratio conditions.

(4) By introducing a time-dependent damage probability function $\Psi(t)$, we simulated the coking behavior of the catalyst over its lifetime and tailored the diameter ratio to maximize the cumulative diffusion flux. Three different $\Psi(t)$ growth curves were considered: when the diameter ratio remained constant, the case where $\Psi(t)$ first increased slowly and then rapidly (Nonlinear 1) maintained high D_e and exhibited the highest cumulative diffusion flux compared to linear growth and the case where $\Psi(t)$ first increased rapidly and then slowly. We systematically evaluated the cumulative diffusion flux under different diameter ratios and demonstrated that tailored diameter ratios can compensate for the damage trend, achieving comparable diffusion performance under the three $\Psi(t)$ scenarios. In this study, the optimized diameter ratios of 0.820 (linear), 0.795 (Nonlinear 1), and 0.835 (Nonlinear 2) resulted in improvements in cumulative diffusion flux of 1.98%, 0.86%, and 3.81%, respectively, compared to the conventional design (ODR = 0.772).

Finally, the existing model can be further refined. While this study assumes a constant branching number ($n = 2$), extending it to variable branch counts would enhance its applicability. Additionally, in real systems, damage occurs at various branch levels, not just terminal branches. Future work should incorporate theoretical design of the diameter ratio across different branch levels to account for such damage.

CRediT Authorship Contribution Statement

Chijin Zhang: Writing – original draft, Methodology, Investigation. Jiawei Teng: Project administration, Funding acquisition. Chuanming Wang: Writing – review & editing, Formal analysis. Zuwei Liao: Funding acquisition, Data curation. Zaiku Xie: Resources, Conceptualization.

Declaration of Competing Interest

The authors declare that they have no known competing financial interests or personal relationships that could have appeared to influence the work reported in this paper.

Acknowledgements

We gratefully acknowledge the financial support provided by the Project of National Key Research and Development Program of China (2023YFA1507700, 2024YFA1509902).

Nomenclature

A_t	diffusion cross-sectional area, m^2
B_i	Boolean variable
c	connectivity parameter
D_e	effective diffusion coefficient of porous media, $m^2 \cdot s^{-1}$
D_e^{opt}	optimal effective diffusion coefficient of porous media, $m^2 \cdot s^{-1}$
D_p	dimensionless pore fractal dimension
D_k	diffusion coefficient for a k-th cylindrical tube, $m^2 \cdot s^{-1}$
D_k^{eff}	effective diffusion coefficient for a k-th cylindrical tube, $m^2 \cdot s^{-1}$
D_t	dimensionless tortuosity fractal dimension
d_e	geometric dimension
d_k	tube diameter, m
d_k^{eff}	effective tube diameter, m
$d_{0,max}$	maximum diameter of the parent tubes, m
$d_{0,min}$	minimum diameter of the parent tubes, m
H_0	total vertical height, m
$\overline{h}$	average height of the roughness elements, m
i	tree-like network number
Kn	Knudsen number
k	branching level index
k_B	Boltzmann constant
k_d	damaged branching level
L_0	effective diffusion length or total horizontal length, m
l_k	tube length, m
M	gas molecular mass, kg
m	total branching level
N_d	number of damaged branches
N_T	total number of tree-like networks at the inlet section
n	branching number
P	pressure, Pa
Q	cumulative diffusion flux per unit area, m^2
Q_i	total flow through the i-th tree-like network, $mol \cdot s^{-1}$
Q_t	total flow through porous media, $mol \cdot s^{-1}$
q_k	gas flow rate through the k-th level branch, $mol \cdot s^{-1}$
R_i	random number
T	temperature, K
V	total pore volume of the porous media, m^3
V_i	sub-volume of the i-th tree-like network, m^3
ΔC_k	concentration difference at the k-th level branch, $mol \cdot m^{-3}$
ΔC_i	total concentration difference, $mol \cdot m^{-3}$
α	length ratio
β	diameter ratio
δ_c	standard deviation of connectivity distribution
ε_k	relative roughness

θ	branching angle
λ	mean free path, m
μ_c	average connectivity
σ	molecular diameter, m
τ_k	tortuosity
ϕ_v	volume porosity
Ψ	damage probability

References

[1] B. Mandelbrot, How long is the coast of Britain? Statistical self-similarity and fractional dimension, *Science* 156 (3775) (1967) 636–638.

[2] B.Q. Xiao, Q.W. Huang, H.X. Chen, X.B. Chen, G.B. Long, A fractal model for capillary flow through a single tortuous capillary with roughened surfaces in fibrous porous media, *Fractals* 29 (1) (2021) 2150017.

[3] B.Q. Xiao, H.Z. Zhu, F.Y. Chen, G.B. Long, Y. Li, A fractal analytical model for Kozeny-Carman constant and permeability of roughened porous media composed of particles and converging-diverging capillaries, *Powder Technol.* 420 (2023) 118256.

[4] B.L. Tu, B.Q. Xiao, Y.D. Zhang, G.B. Long, An analytical model for permeability of fractal tree-like branched networks composed of converging–diverging capillaries, *Phys. Fluids* 36 (4) (2024) 043621.

[5] S.F. Li, J. Gao, B.Q. Xiao, Y.D. Zhang, G.B. Long, Y. Li, Fractal analysis of dimensionless permeability and Kozeny–Carman constant of spherical granular porous media with randomly distributed tree-like branching networks, *Phys. Fluids* 36 (6) (2024) 063614.

[6] P.L. Wang, J. Gao, B.Q. Xiao, G.B. Long, Q. Zheng, D.H. Shou, The fastest capillary flow in root-like networks under gravity, *Langmuir* 40 (18) (2024) 9741–9750.

[7] Q. Zheng, B.M. Yu, S.F. Wang, L. Luo, A diffusivity model for gas diffusion through fractal porous media, *Chem. Eng. Sci.* 68 (1) (2012) 650–655.

[8] Q. Zheng, X.P. Li, Gas diffusion coefficient of fractal porous media by Monte Carlo simulations, *Fractals* 23 (2) (2015) 1550012.

[9] J.H. Yang, M. Wang, L. Wu, Y.W. Liu, S.X. Qiu, P. Xu, A novel Monte Carlo simulation on gas flow in fractal shale reservoir, *Energy* 236 (2021) 121513.

[10] J.C. Cai, D.L. Lin, H. Singh, W. Wei, S.W. Zhou, Shale gas transport model in 3D fractal porous media with variable pore sizes, *Mar. Petrol. Geol.* 98 (2018) 437–447.

[11] J.Z. Xu, K.L. Wu, R. Li, Z.D. Li, J. Li, Q.L. Xu, Z.X. Chen, Real gas transport in shale matrix with fractal structures, *Fuel* 219 (2018) 353–363.

[12] J. Gao, B.Q. Xiao, B.L. Tu, F.Y. Chen, Y.H. Liu, A fractal model for gas diffusion in dry and wet fibrous media with tortuous converging–diverging capillary bundle, *Fractals* 30 (9) (2022) 2250176.

[13] B.Q. Xiao, S. Wang, Y. Wang, G.P. Jiang, Y.D. Zhang, H.X. Chen, M.C. Liang, G.B. Long, X.B. Chen, Effective thermal conductivity of porous media with roughened surfaces by fractal-Monte Carlo simulations, *Fractals* 28 (2) (2020) 2050029.

[14] Z.Z. Yin, Q. Zheng, H.L. Wang, X.Y. Guo, Effective gas diffusion coefficient of fractal porous media with rough surfaces by Monte Carlo simulations, *Fractals* 30 (2022) 2250010.

[15] B.B. Li, J.T. Li, S.D. Ren, S. Gu, Z.J. Liu, L.Y. Liu, Development of a capillary bundle evaporation advanced mathematical modeling for 1, 2-propylene glycol–glycerin mixtures in porous media, *Chin. J. Chem. Eng.* 80 (2025) 261–273.

[16] C.D. Murray, The physiological principle of minimum work: I. the vascular system and the cost of blood volume, *Proc. Natl. Acad. Sci. USA* 12 (3) (1926) 207–214.

[17] M.A. Khan, M. Suhaib, M. Ahmad Ansari, Investigations on fluid flow and mixing in fractal tree like biomimetic microchannel based on Murray's law, *Chem. Eng. Process. Process Intensif.* 194 (2023) 109564.

[18] D.L. Jing, S.Y. Song, Y.L. Pan, X.M. Wang, Optimal fractal tree-like microchannel networks with slip for laminar-flow-modified Murray's law, *Beilstein J. Nanotechnol.* 9 (2018) 482–489.

[19] D. Heymann, D. Pence, V. Narayanan, Optimization of fractal-like branching microchannel heat sinks for single-phase flows, *Int. J. Therm. Sci.* 49 (8) (2010) 1383–1393.

[20] Y.L. Chen, X.Q. Zhang, L.X. Ren, Y.Y. Geng, G.Q. Bai, Analysis of blood flow characteristics in fractal vascular network based on the time fractional order, *Phys. Fluids* 33 (4) (2021) 041902.

[21] H.B. Uylings, Optimization of diameters and bifurcation angles in lung and vascular tree structures, *Bull. Math. Biol.* 39 (5) (1977) 509–520.

[22] X.F. Zheng, G.F. Shen, C. Wang, Y. Li, D. Dunphy, T. Hasan, C.J. Brinker, B.L. Su, Bio-inspired Murray materials for mass transfer and activity, *Nat. Commun.* 8 (2017) 14921.

[23] Y.H. Liu, Z.H. Li, B.Q. Xiao, H.X. Chen, G.B. Long, A novel model for effective thermal conductivity of tree-like branching network with fractal roughened surfaces, *Fractals* 29 (6) (2021) 2150165.

[24] Q. Zheng, H.L. Wang, X.Y. Guo, Research on the effect of surface roughness on gas diffusion coefficient of porous media embedded with a fractal-like tree network, *Fractals* 29 (7) (2021) 2150195.

[25] B.Q. Xiao, P.L. Wang, J.S. Wu, H.Z. Zhu, M.X. Liu, Y.H. Liu, G.B. Long, A novel fractal model for gas diffusion coefficient in dry porous media embedded with a damaged tree-like branching network, *Fractals* 30 (7) (2022) 2250150.

[26] B.Q. Xiao, J. Fang, G.B. Long, Y.Z. Tao, Z.J. Huang, Analysis of thermal conductivity of damaged tree-like bifurcation network with fractal roughened surfaces, *Fractals* 30 (6) (2022) 2250104.

[27] B.W. Hu, J.G. Wang, Z.G. Ma, S.X. Sang, Permeability and thermal conductivity models of shale matrix with a bundle of tortuous fractal tree-like branching micropore networks, *Int. J. Therm. Sci.* 164 (2021) 106876.

[28] S.W. Tang, A.H. B, P. Yu, L. Wang, R.J. Cai, e. Chen, The analysis of thermal resistance of three-dimensional fractal networks embedded in a sphere, *Fractals* 26 (3) (2018) 1850036.

[29] D.L. Jing, L. He, X.M. Wang, Optimization analysis of fractal tree-like microchannel network for electroviscous flow to realize minimum hydraulic resistance, *Int. J. Heat Mass Tran.* 125 (2018) 749–755.

[30] M.C. Liang, Y.H. Gao, L. Luo, B.Q. Xiao, M.H. Pang, Z.K. Wang, A study on the permeability for the tree-like branching network with polygonal loops based on the fractal network of leaf vein, *Chem. Eng. Sci.* 207 (2019) 911–928.

[31] Y.D. Zhang, B.Q. Xiao, B.L. Tu, G.Y. Zhang, Y.B. Wang, G.B. Long, Fractal analysis for thermal conductivity of dual porous media embedded with asymmetric tree-like bifurcation networks, *Fractals* 31 (5) (2023) 2350046.

[32] B.H. Zhou, Q. Cheng, Z. Chen, Z.S. Chen, D.F. Liang, E.A. Munro, G.L. Yun, Y. Kawai, J.R. Chen, T. Bhowmick, K.K. Padmanathan, L.G. Occhipinti, H. Matsumoto, J.W. Gardner, B.L. Su, T. Hasan, Universal Murray's law for optimised fluid transport in synthetic structures, *Nat. Commun.* 15 (1) (2024) 3652.

[33] E.A. Mason, A.P. Malinauskas, Gas Transportin Porous Media: the dusty-gas Model, Elsevier, Amsterdam, 1983.

[34] J.R. Welty, G.L. Rorrer, D.G. Foster, Fundamentals of Momentum, Heat, and Mass Transfer, J. Wiley, Hoboken, 2019.

[35] J. Crank, The Mathematics of Diffusion, Oxford University Press, Oxford, 1979.

[36] S.S. Yang, M.C. Liang, B.M. Yu, M.Q. Zou, Permeability model for fractal porous media with rough surfaces, *Microfluid. Nanofluid.* 18 (5) (2015) 1085–1093.

[37] B.M. Yu, J.H. Li, A geometry model for tortuosity of flow path in porous media, *Chin. Phys. Lett.* 21 (8) (2004) 1569.

[38] J.A. Currie, Gaseous diffusion in porous media. Part 2. - dry granular materials, *Br. J. Appl. Phys.* 11 (8) (1960) 318–324.

[39] B.M. Yu, J.H. Li, Some fractal characters of porous media, *Fractals* 9 (3) (2001) 365–372.

[40] B.M. Yu, Fractal character for tortuous streamtubes in porous media, *Chin. Phys. Lett.* 22 (1) (2005) 158.

[41] J. Comiti, M. Renaud, A new model for determining mean structure parameters of fixed beds from pressure drop measurements: application to beds packed with parallelepipedal particles, *Chem. Eng. Sci.* 44 (7) (1989) 1539–1545.

[42] P. Xu, B.M. Yu, Developing a new form of permeability and Kozeny–Carman constant for homogeneous porous media by means of fractal geometry, *Adv. Water Resour.* 31 (1) (2008) 74–81.